Inishowen Technology Limited
Umricam,
Buncrana,
County Donegal,
Republic of Ireland F93 P8H0

VAT number: IE6591695S

Magnetometer Report for Magheroraty Approaches



Inishowen Technology Limited is incorporated in the Republic of Ireland since 1992.
Company Number 191695

Telephone : +353 74 9363104
E-Mail: sales@iotech.ie

Contents

Contents 2
1. Introduction 3
2. Summary 4
Instrument and Methodology 4
3. Orientation 4
4. Underlying Geology 5
Tellus Data 6
Tellus Magnetic 2018 6
Tellus Radiometric Data 8
5. Fixed Magnetometer Verification 9
6. Survey Activity 10
Reporting 10
Overviews 11
Line M-N1 13
Line M-S2 14
Line M-N3 15
Line M-S4 17
Line M-N5 18
Line M-S6 19
Line M-N7 20
Line M-S22 21
Line M-S20 22
Line M-S10 23
Line M-N11 24
Line M-S12 25
Line M-N13 26
7. References 27

1. Introduction

This report is intended to fulfil the requirements for magnetometer survey as specified in the tender documents "Magheraroarty Approach Channel Survey", October 2019. It is one of a family of four reports.

1. Summary and Interpretative Report
2. Bathymetric Report for Magheraroraty Approaches
3. Side Scan Report for Magheraroraty Approaches
4. Magnetometry Report for Magheraroraty Approaches

This report is a summary only and is accompanied by high resolution copies of all figures and data extracts as specified below.

Donegal County Council requirements were specified as:

1. A mosaic of the search box with anomalies and features identified.

The following deliverables were specified:

1. A summary and interpretive report.
2. A model indicating total field, sufficient to identify and distinguish between topographical and artefactual anomalies.
3. Georeferenced contour charts of magnetic field strength with anomalies indicated and labelled.
4. A georeferenced chart showing survey lines.
5. Profiles of each survey line with anomalies indicated and labelled.

The measurements specified above are carried out in the context of the Works Requirements, Description of Works for this project.

"*Access to Magheraroarty pier has ever more been challenging due to the shallow approach and continuous siltation within the berthing area of the pier. Annual dredging is required to maintain navigable depths at the pier, however, there is also a difficulty on the final approach to the pier where Donegal Co. Council would now like to obtain an accurate profile of the approach channel.*

It is proposed to carry out a number of surveys to determine the most suitable approach route and from this provide Aids to Navigation. Donegal Co. Council would also like to determine the profile and make-up of the sea bed in this area to establish whether or not it is possible to dredge the access channel to make the pier accessible at all levels of tide".

2. Summary

Instrument and Methodology

The magnetometer is towed as it cannot be operated adjacent to any ferro-magnetic material, such as a boat engine. As it is towed, it cannot be safely operated in water <=2m above LAT. The vessel's own navigation system is used as an altimeter and for position and heading data. Post-processing, geomagnetic conditions are verified from fixed monitoring stations (e.g. Inter Magnet, Valentia). The effective use of a magnetometer and the quality of any data is dependent on the underlying geology and on the presence of any ferromagnetic material of artefactual origin. An examination of the most recent aero-magnetic survey data does not raise any obvious issues.

The instrument is a proton magnetometer, and the absolute sensitivity, accuracy and resolution of the instrument is 1nT.

3. Orientation

For detailed orientation information, see the accompanying Interpretive Report. Figure 1 shows the survey area in the context of its wider hinterland, c. 8km x 8km.

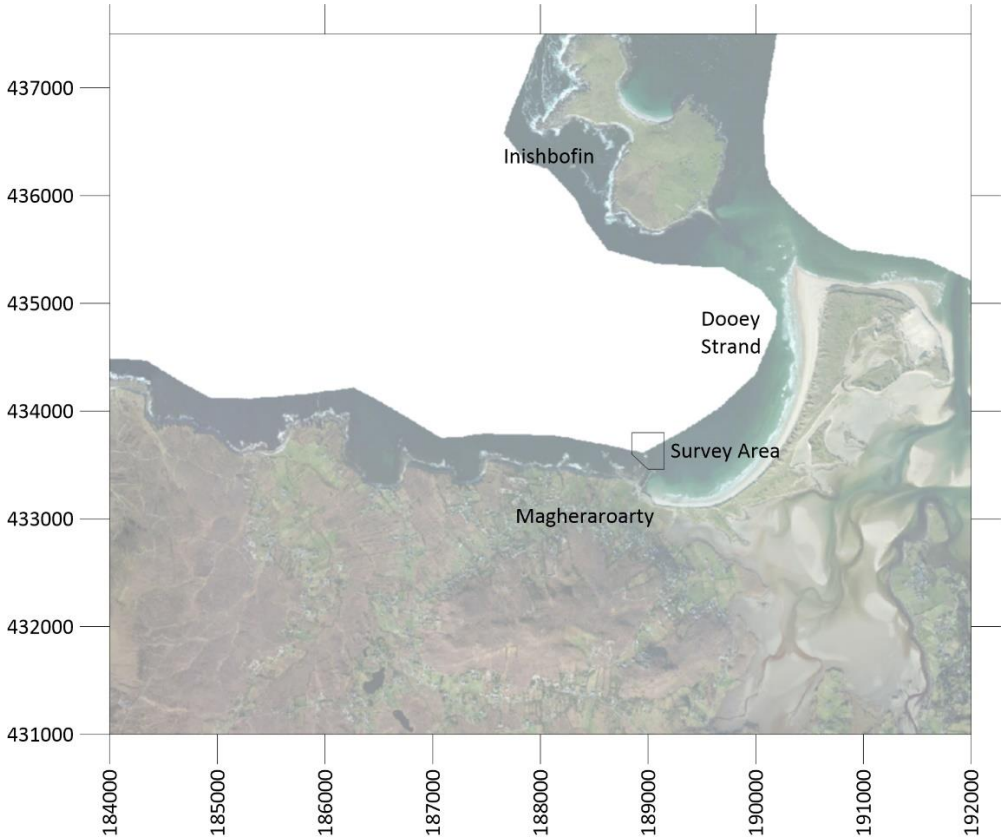


Figure 1. Wide area orientation - Aerial View (OSI)

4. Underlying Geology

A basic understanding of the geology of an area is a critical first step in any magnetometer investigation. The geology of the harbour area is complex, with the Thorr Granite to the south-west with associated Appinite. To the south-east lies the Cresslough Succession. The area has complex faulting, with the Ardsbeg Slide to the east of Figure 6 (line with square dots).

The underlying bedrock of the survey area is undifferentiated/appinite and unfortunately, despite a detailed description [4, Page 40) there may be complex lithography. The appinite suite are derived from magma formed under high water vapour pressure and may have a composition high in ferrous oxide, significant for magnetometer measurements.

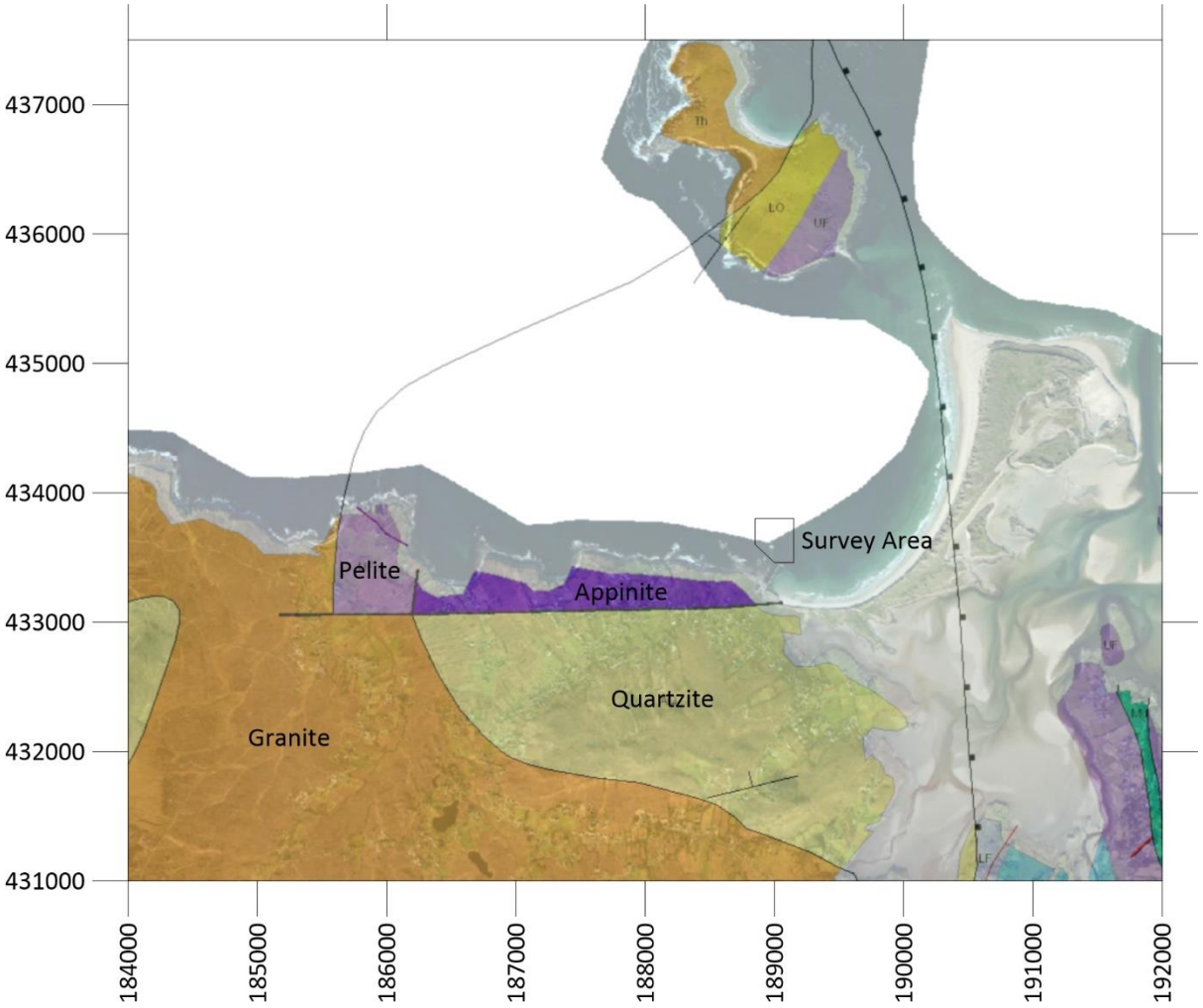


Figure 2. Geology of the wide area (GSI) overlaying aerial photography (OSI)

Tellus Data

The Tellus project was established by the GSI to gather geochemical and geophysical data across Ireland. Data from airborne surveys in 2018 has been made publicly available.

Tellus Magnetic 2018

One of the most useful reconnaissance tools is to make measurements of slight variations in the Earth's magnetic field. In very simple terms, a magnetic monopole (an isolated high or low) normally indicates a geological feature. A magnetic dipole (a swing between low and high) normally indicates an artefact of ferromagnetic material. In an area of such geological diversity, this can be a useful indicator of the borders of bedrock bodies.

In Figure 3, the pier is clearly identifiable as a magnetic dipole, just south of the survey area. West of the survey area, some interesting features indicate geological structures not showing in the bedrock data. However, the survey area appears to show homogeneity.

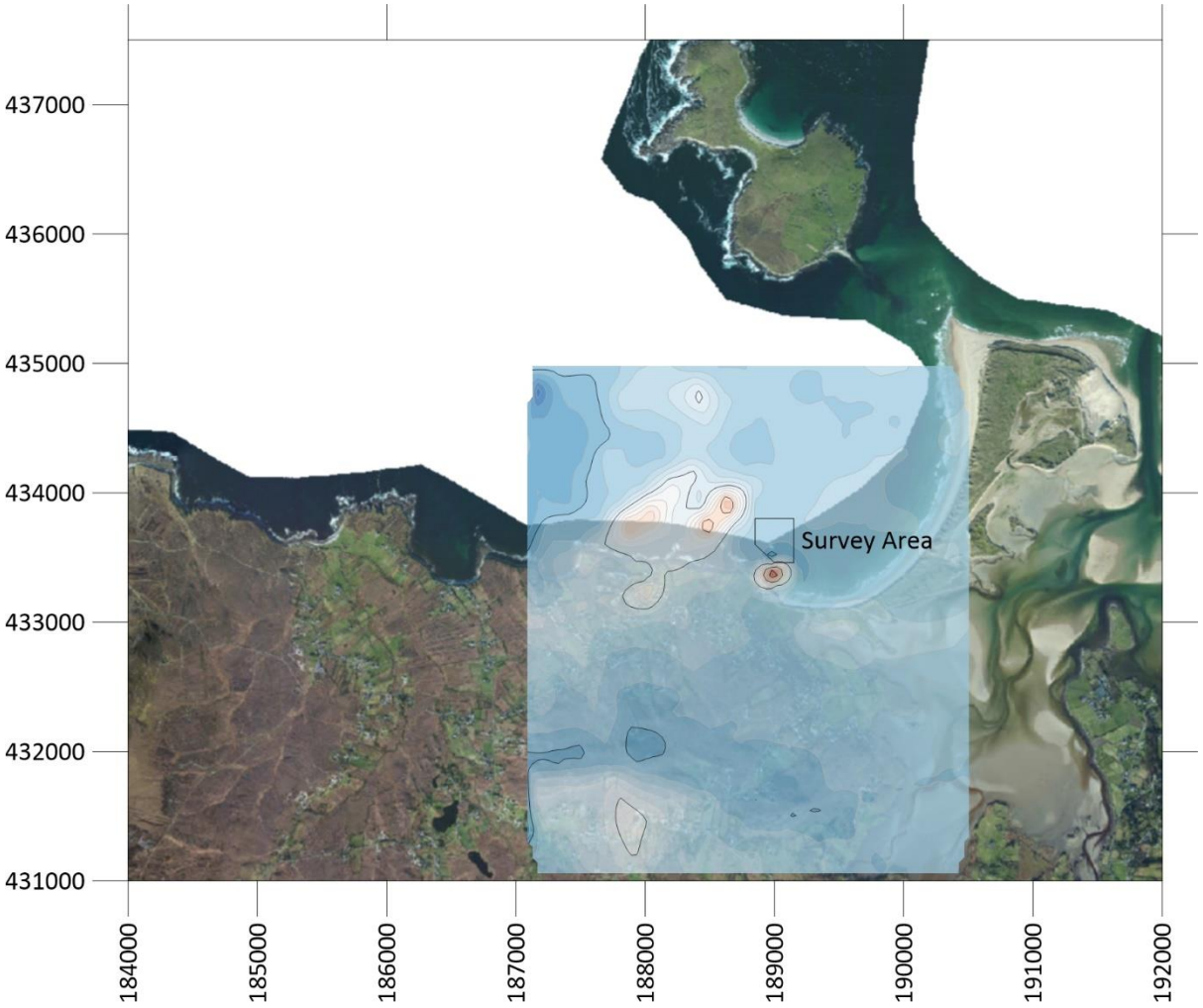


Figure 3. Wide Area, Aerial photography (OSI) and Tellus Magnetic Data 2018

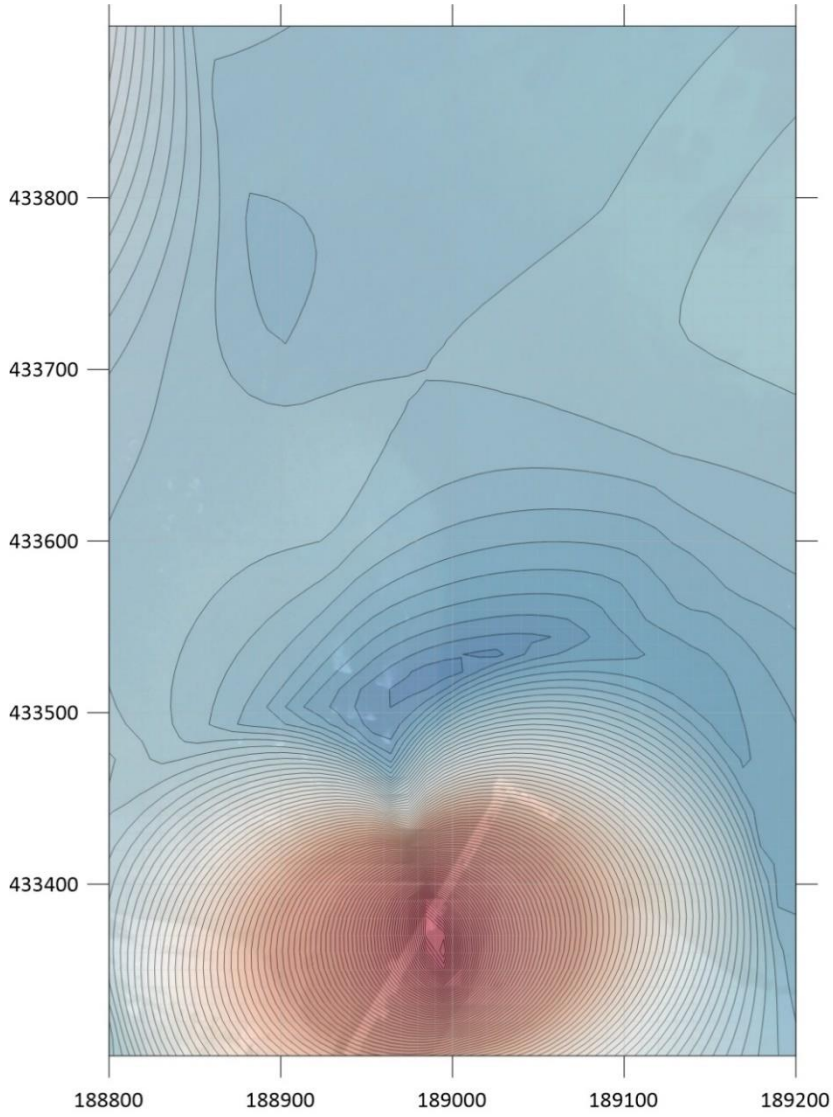


Figure 4. Survey Area, Aerial photography (OSI) and Tellus Magnetic Data 2018

As can be seen, the ferromagnetic material associated with the pier overwhelms any local signal. If the seabed were sand, it would be possible to extract useful information from individual lines. However as commented in section 4, the underlying rock is ferromagnetic and at close range (2-4m) this results in measurements of limited utility.

Tellus Radiometric Data

Airborne geophysical Gamma-Ray data for Potassium (Figure 5), Thorium (Figure 6) and Uranium (Figure 7) may also provide hints as to the boundaries of bedrock bodies on land.

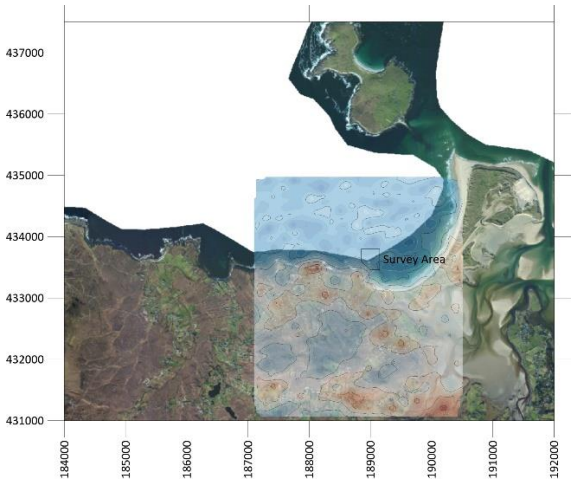


Figure 5. Aerial photography (OSI) and Tellus Radiometric (Potassium)

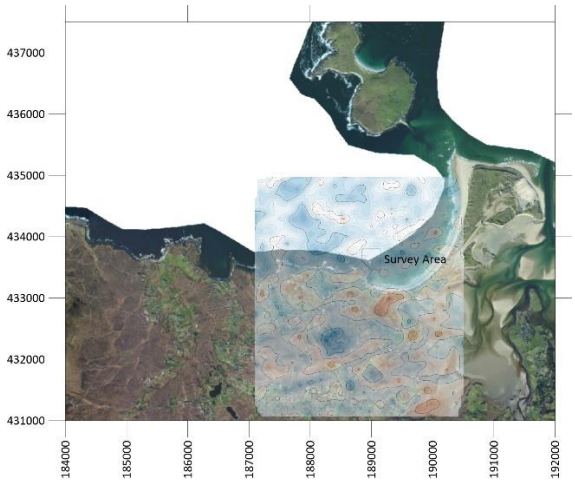


Figure 6. Aerial photography (OSI) and Tellus Radiometric (Thorium)

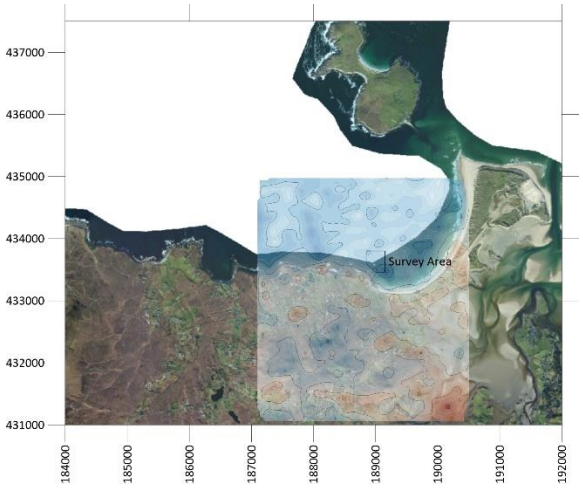


Figure 7. Aerial photography (OSI) and Tellus Radiometric (Uranium)

5. Fixed Magnetometer Verification

A magnetometer uses local variations in the earth's magnetic field to identify cultural artefacts and underlying geology. To quality assure data, it is customary to process fixed data from earth observation stations, to allow for natural variations in the Earth's magnetic field. For example, diurnal variations are associated with the Sun and to a lesser extent, the Moon.

In Ireland, the MagIE project [1] provides archival data from the observatory in Valentia. Recordings are reported in three axes (X, Y, Z) and total field is calculated by applying Pythagoras Theorem in three dimensions to solve for the hypotenuse.

$$B_{Total} = \sqrt{B(x)^2 + B(y)^2 + B(z)^2}$$

Figure 8 shows plot data for the 18th September 2020.

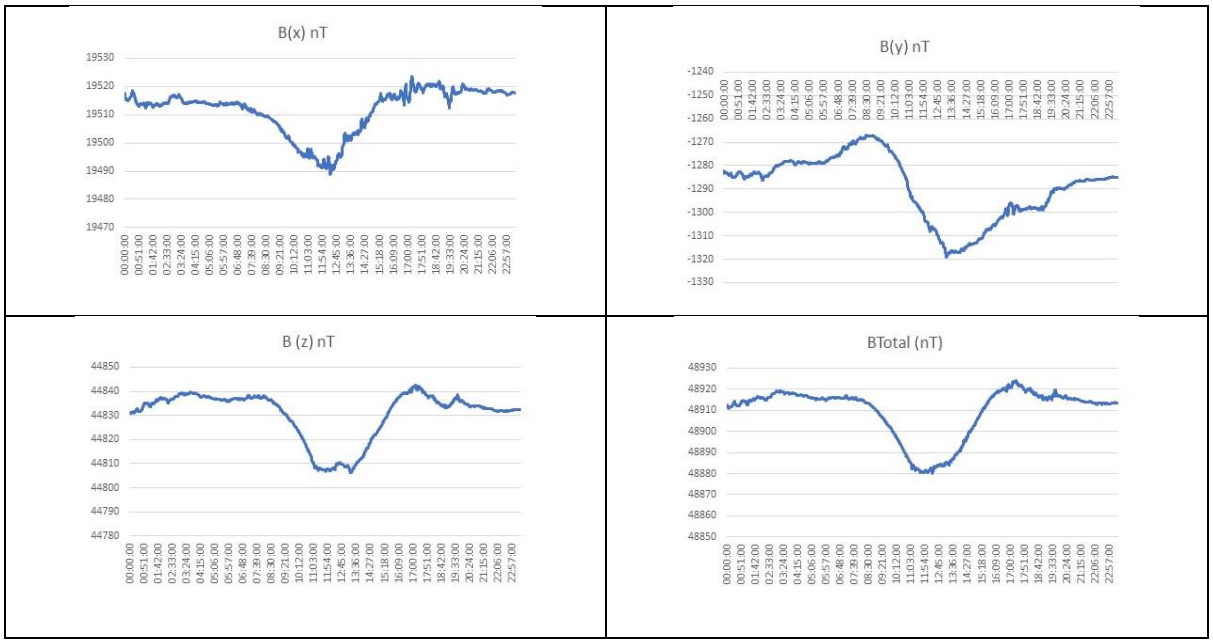


Figure 8. Magnetometer data from Valentia 18th September 2020

Active survey data was taken between 1606 and 1914, when the underlying field at this latitude was stable, variations in this time are given in Table 1. The variation of 8nT is far less than the variations due to local geology and can be ignored.

	Total Field (nT)	Delta
Max	48923.98	4.3298
Median	48919.65	
Min	48915.17	4.4885

Table 1. Total field statistics during the survey activity

6. Survey Activity

1. Lines were taken on 18th September 2020.
2. For safety, due to the shallow nature of much of the survey area, the tow-fish was suspended from a buoy c. 1m below the surface.
3. The magnetometer cannot be operated adjacent to any ferromagnetic material. The tow-fish was operated from a 10m line and layback is calculated for and compensated for on each line.
4. East-West lines were taken with c. 20m spacing for cross verification only.
5. North-South lines were taken with c. 10m spacing and were interlaced, due to the turning circle with a 10m tow-fish
6. For reconnaissance, samples were taken every 3 seconds. With a survey speed c. 1m/s this leads to a sample every c. 3m along each survey line.
7. Lobster pots close to survey point D prevented operating the tow fish around this point. See Figure 8.

Reporting

1. All data points are identified by a UTC time stamp, in seconds.
2. In the lines analysis to avoid repetition:
    a. Every second line is analysed in detail
    b. EW lines were for cross-check and verification and are not shown.
3. 2D and 3D overviews are provided.
4. All data has been provided to the client in CSV format.



Figure 9. Magnetometer NS coverage showing c. 1/10th of measurements

Overviews

A contour chart of the NS magnetometer data is provided in Figure 10. The ferromagnetic material associated with the pier causes a high total field reading in the south of the chart. There are linear features associated with the channel, this is an artefact of the depth to bedrock and is otherwise not of interest.

There is a positive anomaly (red) marked. This shows on three adjacent lines, but the monopole nature of the anomaly suggests geology rather than a cultural artefact. A detailed search of the side-scan traces close to 189077, 433658 show a number of boulders, but no significant surface feature.

Other anomalies are smaller in nature and are primarily related to the underlying geology and the distance from the magnetometer instrument to the seabed.

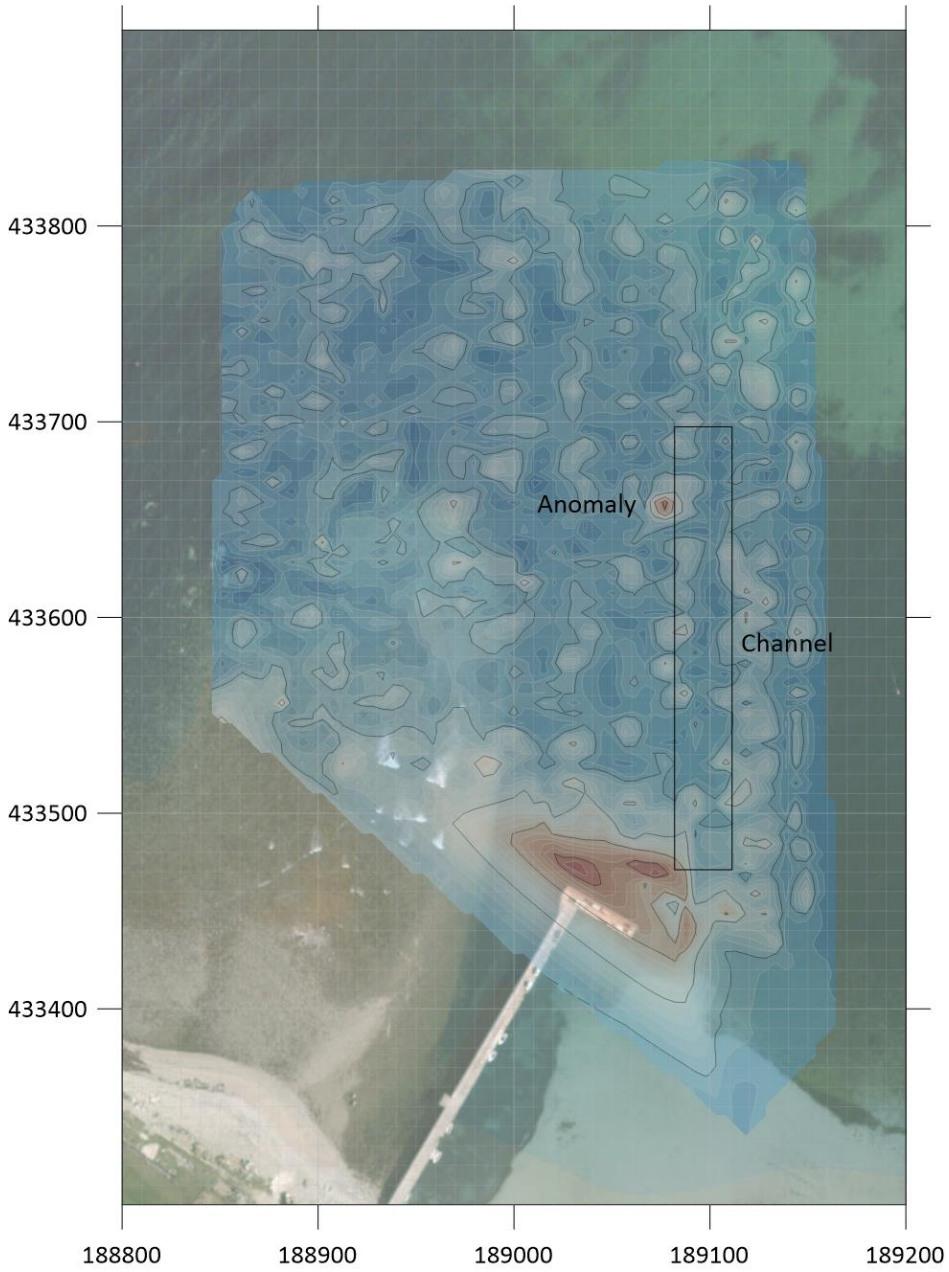


Figure 10. 2D Survey Area Aerial Photography (OSI) overlayed with NS Magnetometer

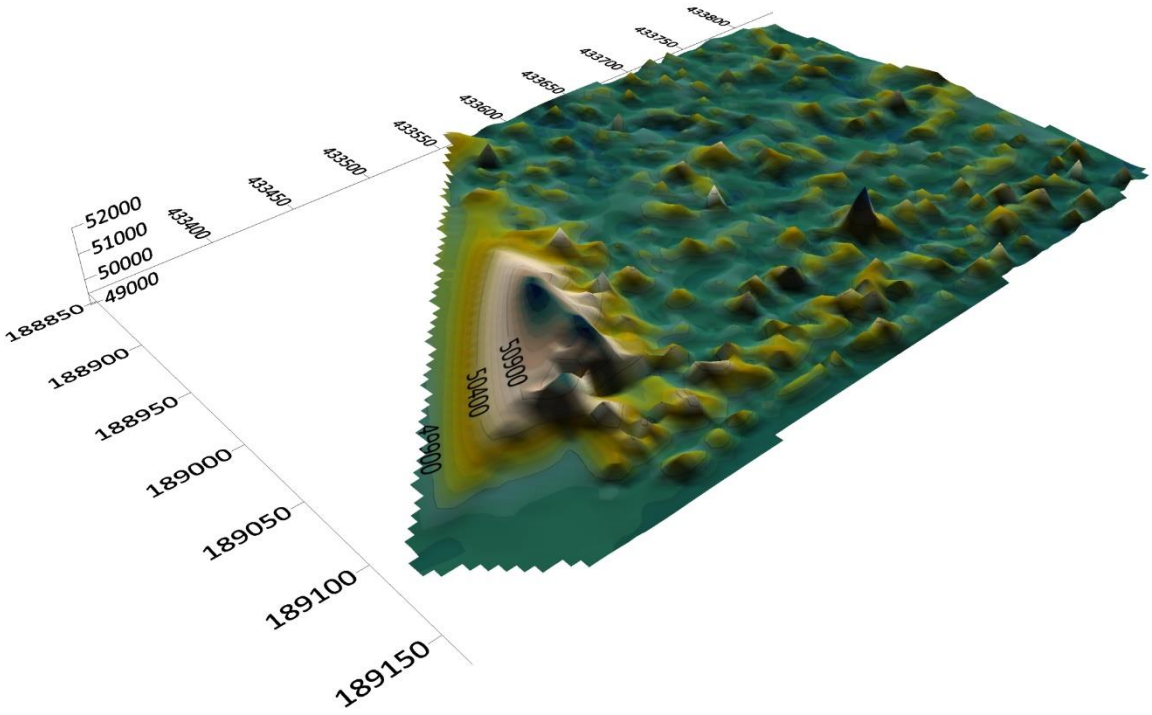


Figure 11. 3D Survey Area with NS Magnetometer viewed from South-East

Figure 11 gives a 3D representation of the survey area looking from the south-west. The linear associated with the channel is clear, as is the noted anomaly. The anomalies are of a geological nature and are not considered significant.

Line M-N1

Direction	North	
Layback	-10	Metres
Max	49759	nT
Median	49662	nT
Min	49553	nT
Start	160651	UTC
Finish	161446	UTC

Table 2

The most easterly line (Figure 12) runs north on a line at 189150. Shows the distant influence of the pier.

Line M-N1 (Figure 13) otherwise demonstrates geological variations. Lobster pots/chains may show at c. 1608. There are no significant features of interest.

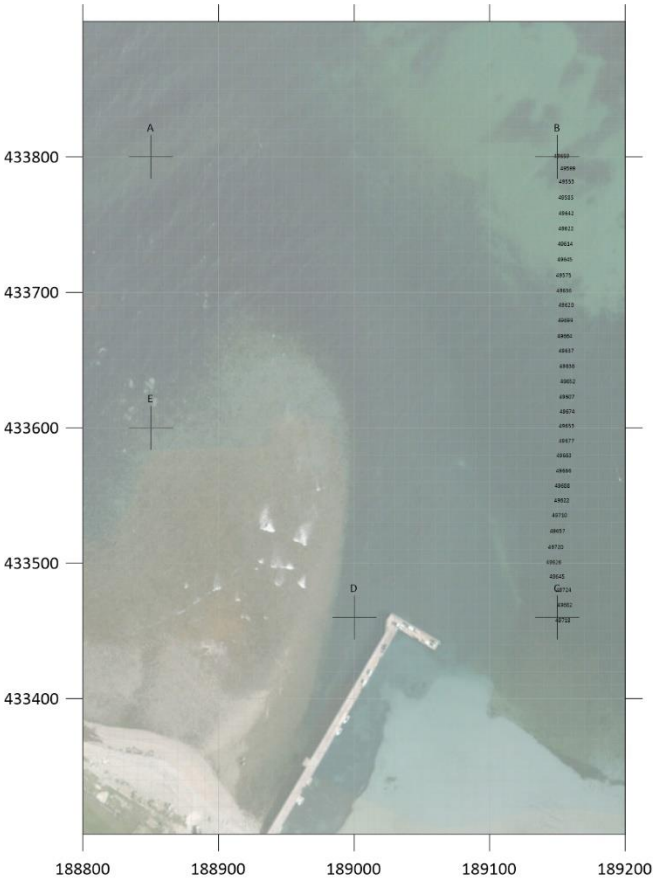


Figure 12

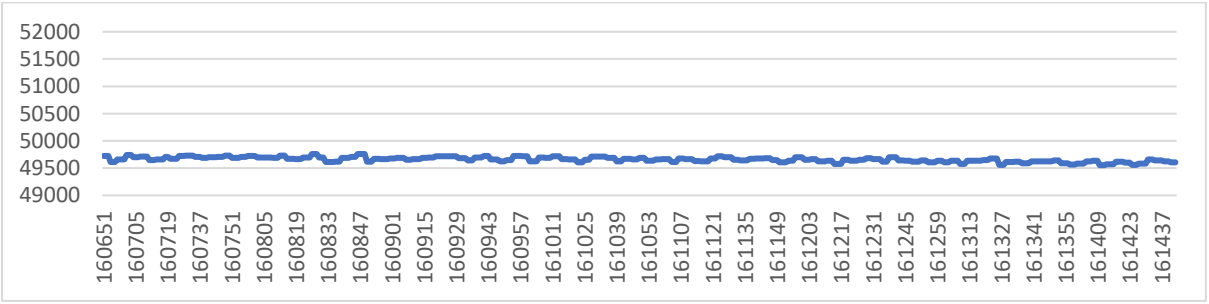


Figure 13. Line M-N1

Line M-S2

Direction	South	
Offset	10	Metres
Max	51101	nT
Median	49675	nT
Min	49566	nT
Start	161501	UTC
Finish	162052	UTC

Table 3

Line M-S2 (Figure 14) runs south on a line at c. 189120 but is skewed to avoid an egressing vessel. The much closer approach to the pier shows a distinctive increase in total field.

This line (Figure 15) otherwise demonstrates geological variations.

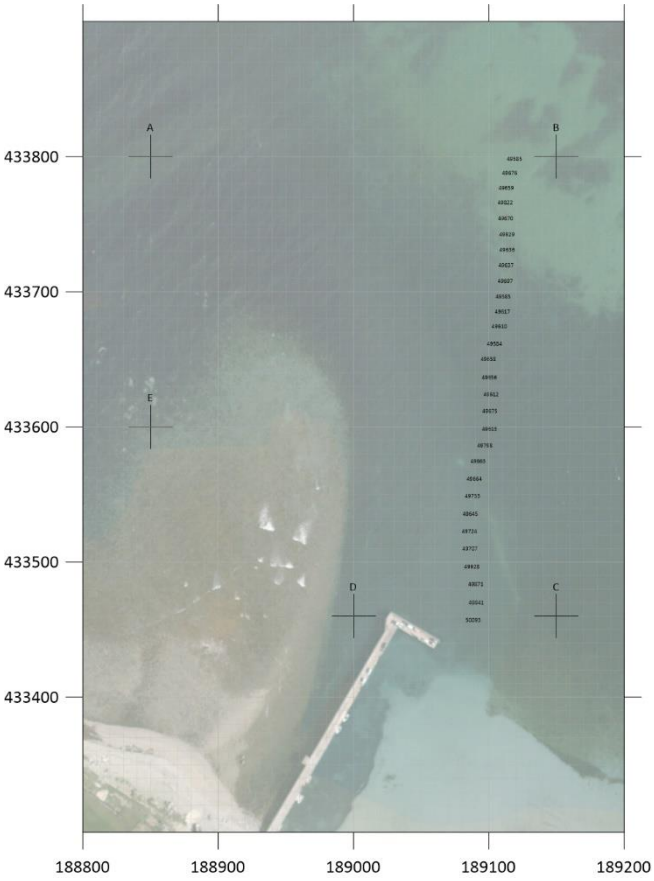


Figure 14

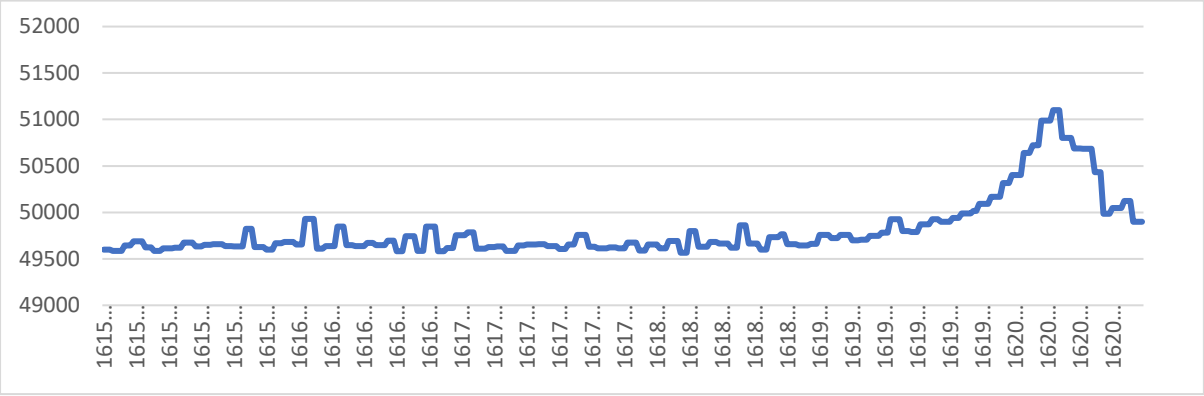


Figure 15. Line M-S1

Line M-N3

Direction	North	
Offset	-10	Metres
Max	49897	nT
Median	49678	nT
Min	49509	nT
Start	162105	UTC
Finish	162647	UTC

Table 4

The influence of the pier is just discernible at the start of the line (Figure 17) which runs north around 189140.

This line (Figure 16) runs over the east wall of the channel and the southern portion of the track is shallow and otherwise demonstrates geological variations.

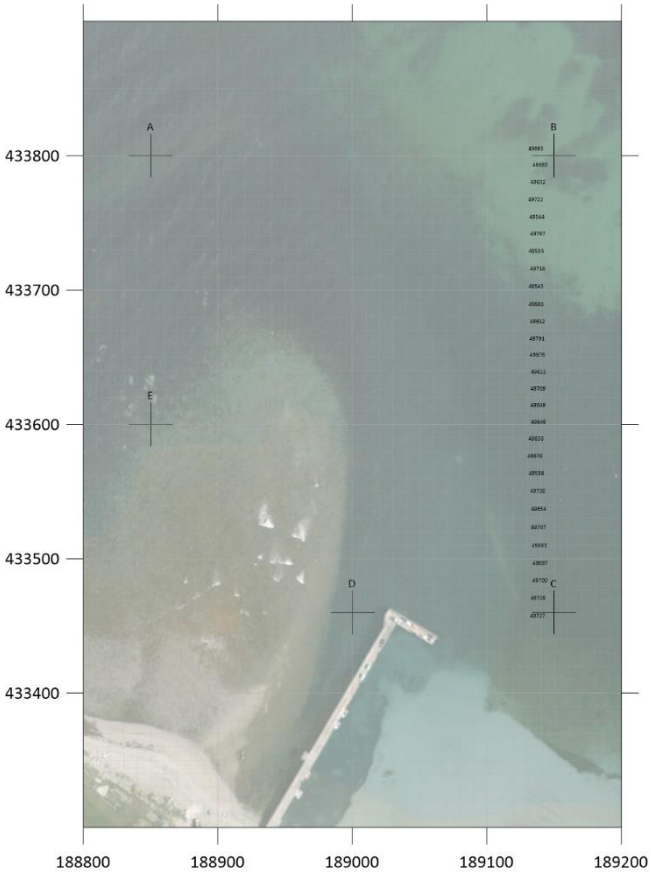


Figure 16

The anomaly at 162225 (189137, 433498) was cross checked with sonar (Figure 18) and side-scan (Figure 19). This corresponds to a boulder at the slope to the channel.

Lobster pots/chains around mid-way through the line may show from 162415, there are otherwise small boulders at this point, no other objects of significance.

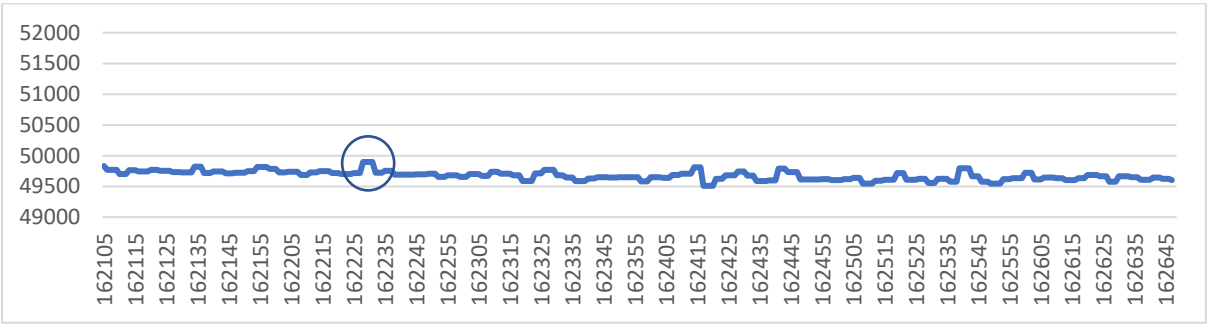


Figure 17. Magnetometer trace for line M-N3

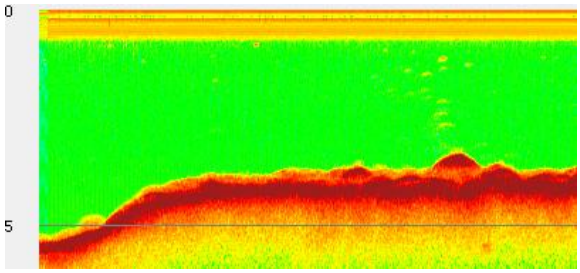


Figure 18. Sonar at 189137, 433498

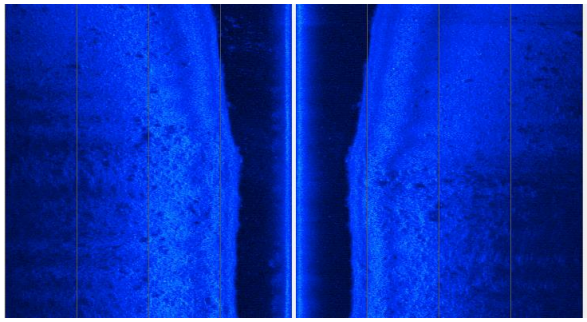


Figure 19. Side-scan Sonar at 189137, 433498

Line M-S4

Direction	South	
Offset	10	Metres
Max	50271	nT
Median	49655	nT
Min	49516	nT
Start	162658	UTC
Finish	163140	UTC

Table 5

The influence of the pier is discernible at the end of the line (Figure 21) which is centred on 189100. This line (Figure 20) runs through the centre of the channel and the variations around 1630 mark the transition ridge, the shallowest point on this line.

The southern portion of the track is also shallow and otherwise demonstrates geological variations.

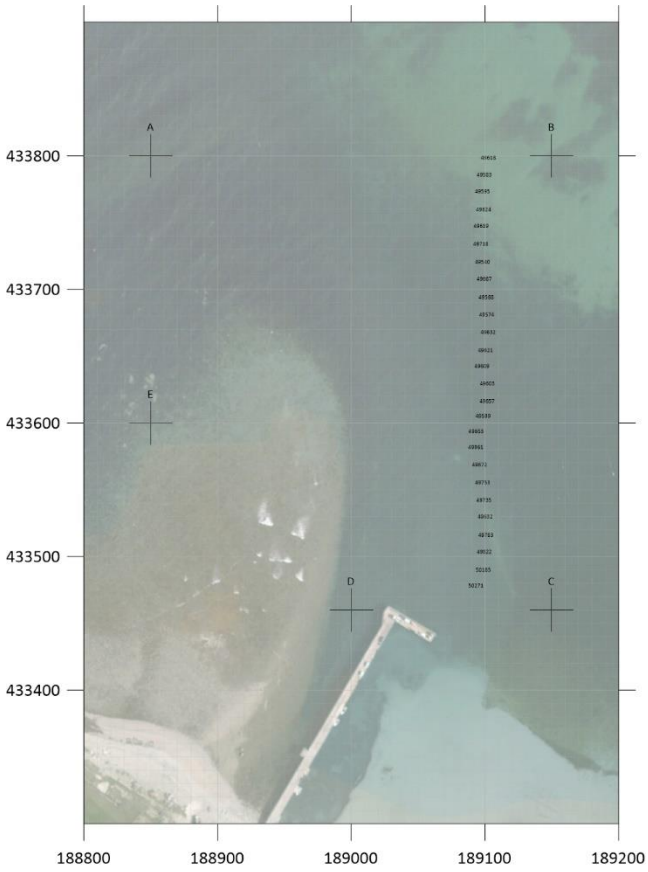


Figure 20

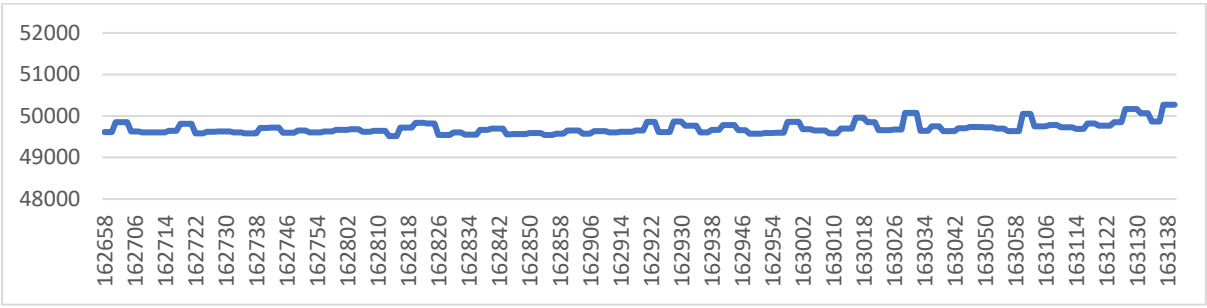


Figure 21. Line M-S4

Line M-N5

Direction	North	
Offset	-10	Metres
Max	51521	nT
Median	49710	nT
Min	49530	nT
Start	163144	UTC
Finish	163621	UTC

Table 6

Line M-N5 (Figure 22) runs over the west wall of the channel centred around 189070. The close approach to the pier shows a distinctive increase in total field in the south of the line (Figure 23).

This line otherwise demonstrates geological variations.

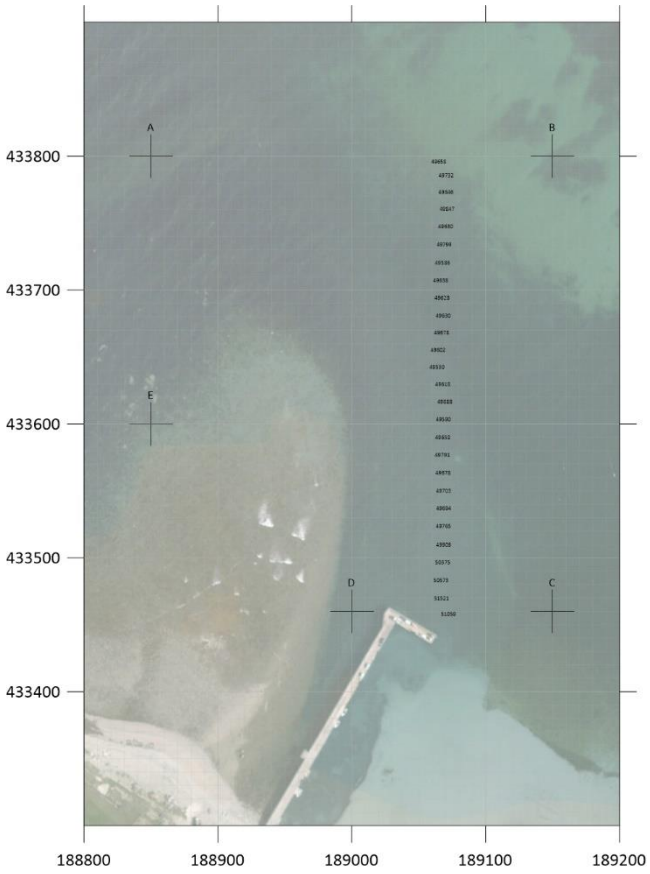


Figure 22

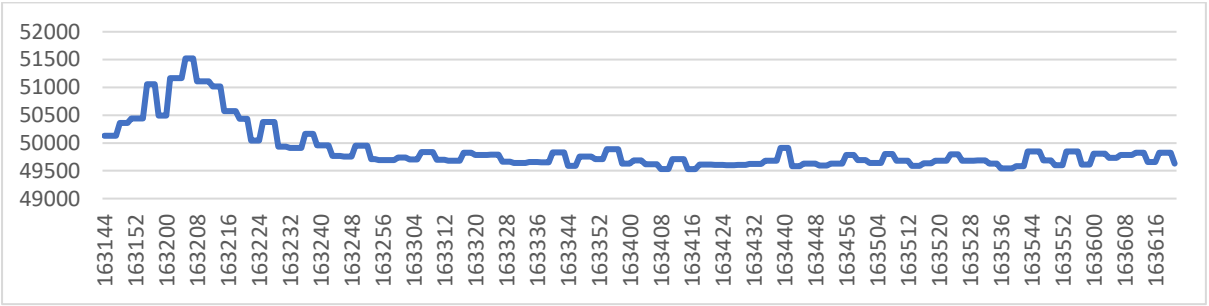


Figure 23. Line M-N5

Line M-S6

Direction	South	
Offset	10	Metres
Max	50590	nT
Median	49670	nT
Min	49536	nT
Start	163631	UTC
Finish	164039	UTC

Table 7

The influence of the pier is significant at the end of the line (Figure 23) which is centred on 189050. This line (Figure 22) runs over the west wall of the channel.

The track otherwise demonstrates geological variations.

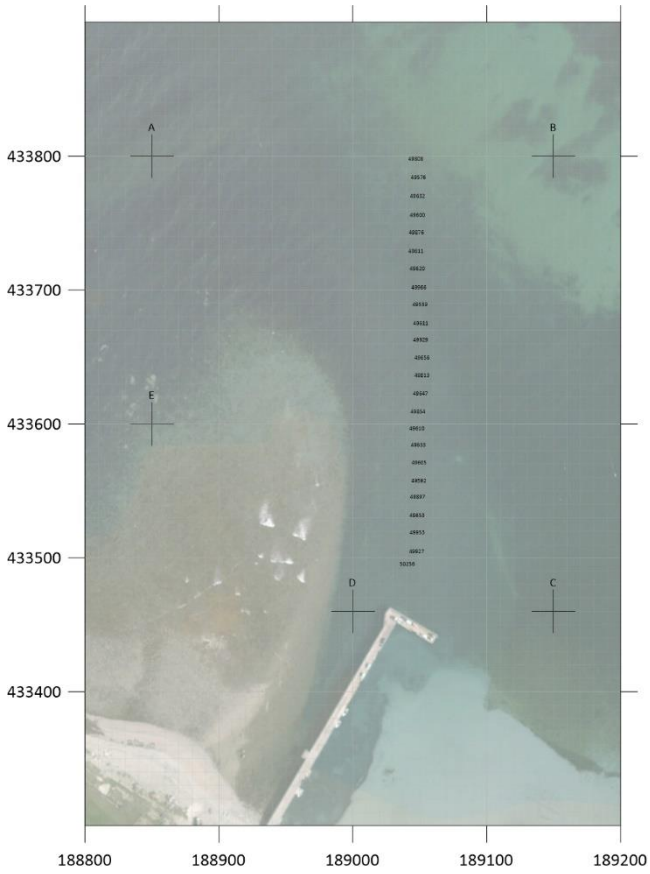


Figure 24

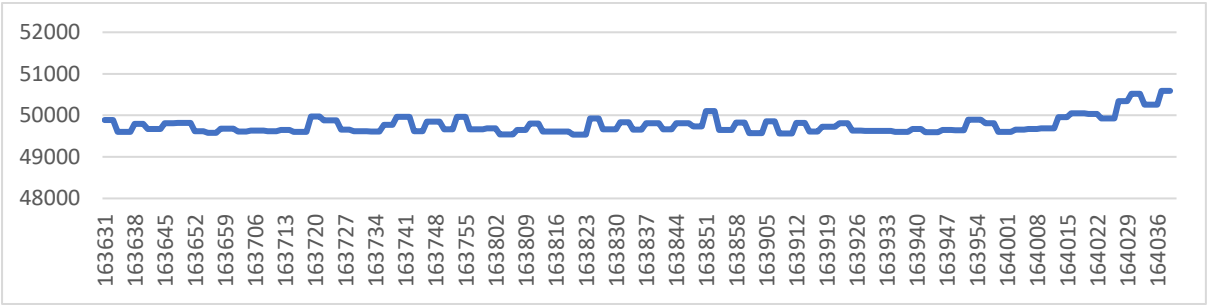


Figure 25. Line M-S6

Line M-N7

Direction	North	
Offset	-10	Metres
Max	51643	nT
Median	49737	nT
Min	49471	nT
Start	164045	UTC
Finish	164459	UTC

Table 8

Line M-N7 (Figure 26) runs west of the channel centred around 189020. The close approach to the pier shows a distinctive increase in total field in the south of the line (Figure 27).

This line otherwise demonstrates geological variations.

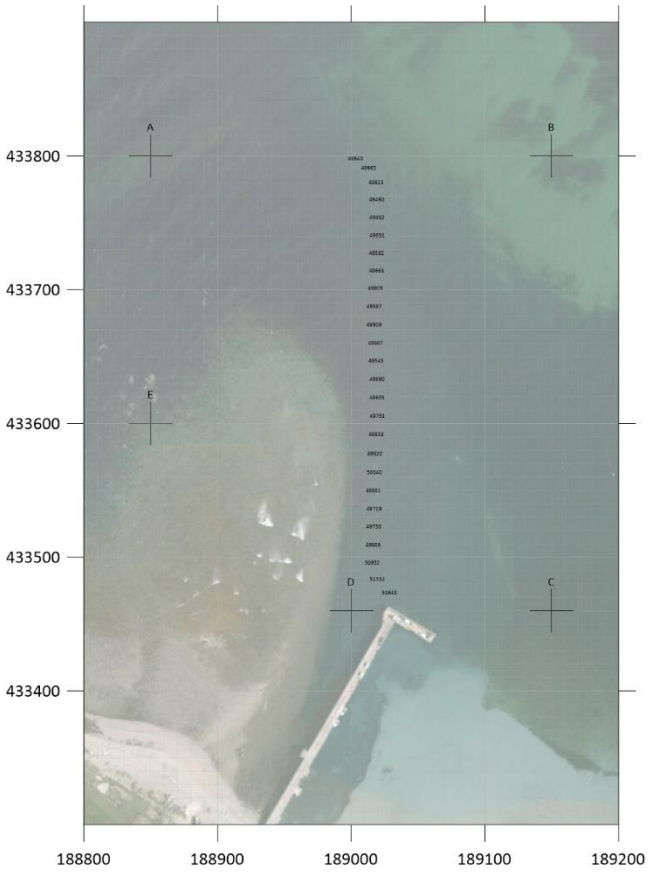


Figure 26

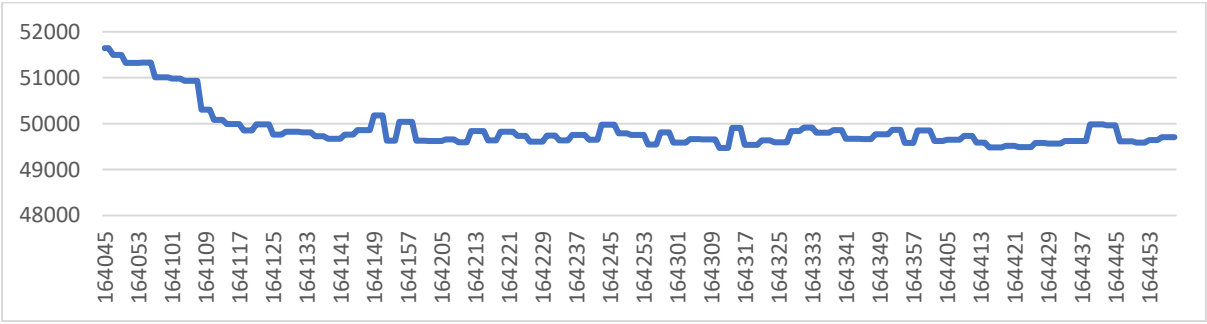


Figure 27. Line M-N7

Line M-S22

Direction	South	
Offset	10	
Max	50781	nT
Median	49907	nT
Min	49434	nT
Start	173623	UTC
Finish	173952	UTC

Table 9

Line 8 was curtailed due to breaking waves at the reef. Line M-S22 covers almost the same zone, centring on 188970 (Figure 28). A slight rise in total field at the end of the line (Figure 29) represents the pier.

This line is entirely over the reef and otherwise demonstrates geological variations. An examination of sonar and side-scan on the north of the line shows many small boulders but no specific features.

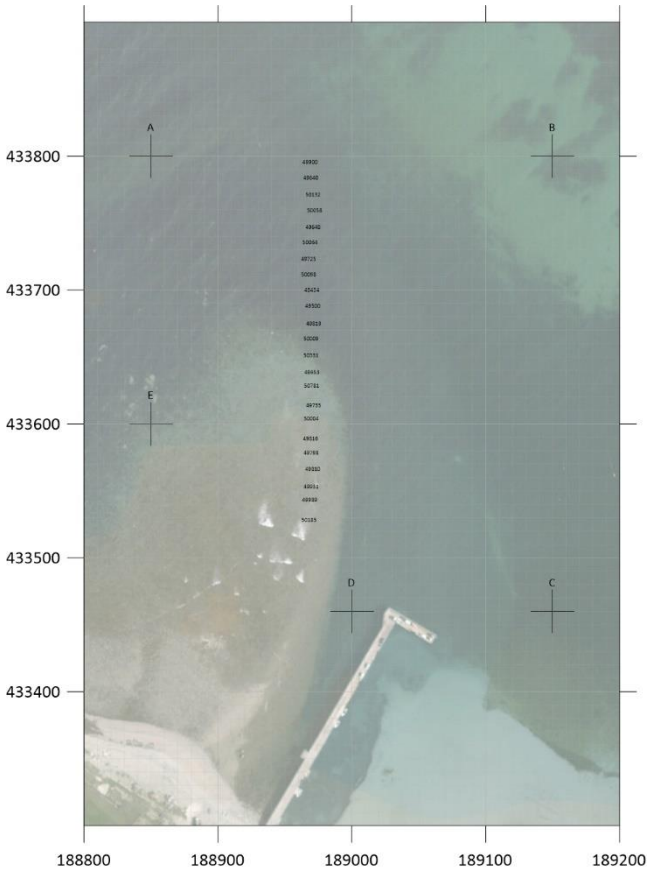


Figure 28

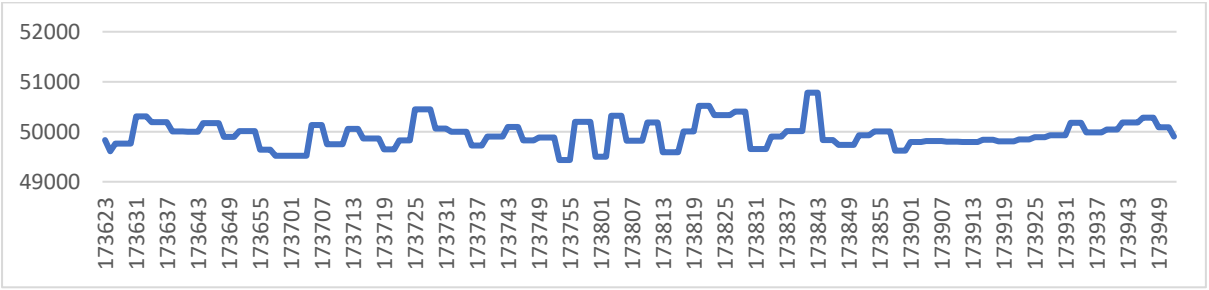


Figure 29. Line M-S22

Line M-S20

Direction	South	
Offset	10	Metres
Max	50328	nT
Median	49785	nT
Min	49494	nT
Start	172854	UTC
Finish	173244	UTC

Table 10

Line 9 followed line 8 and was curtailed due to breaking waves at the reef. Line M-S20 covers almost the same zone, centring on 188930 (Figure 30). This line (Figure 31) is entirely over the reef and demonstrates geological variations.

An examination of sonar and side-scan shows no specific features.

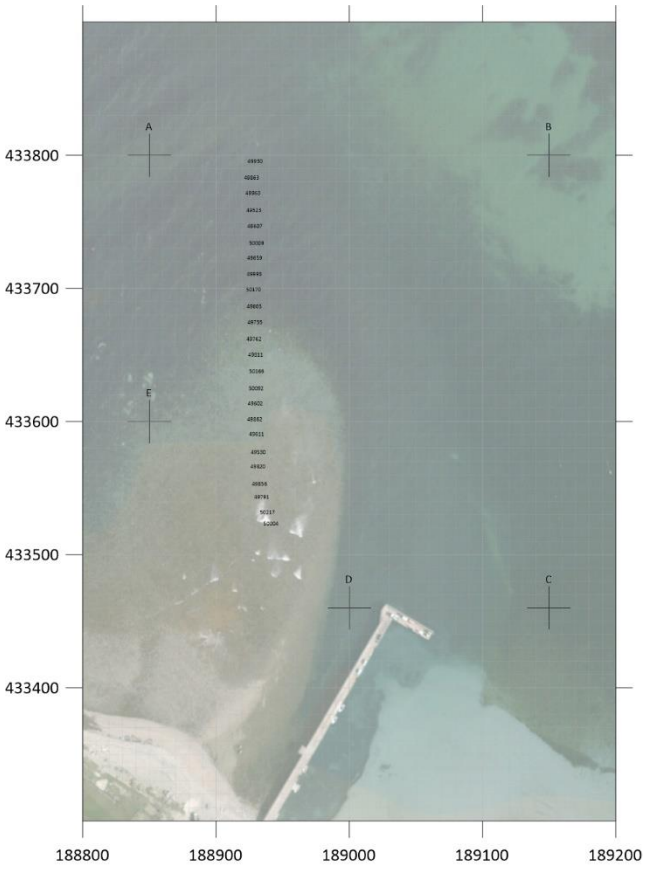


Figure 30

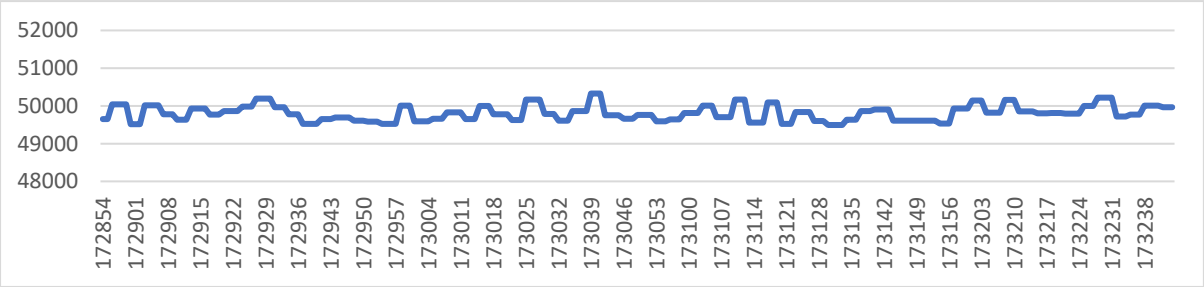


Figure 31. Line M-S20

Line M-S10

Direction	South	
Offset	10	Metres
Max	50366	nT
Median	49704	nT
Min	49464	nT
Start	165115	UTC
Finish	165507	UTC

Table 11

Line M-S10 centres on 188920 (Figure 30). This line (Figure 31) is entirely over the reef and demonstrates geological variations.

The anomaly at 1653 (188909, 433634) was cross checked with sonar (Figure 32) and side-scan (Figure 33) and represents a boulders and exposed bedrock.

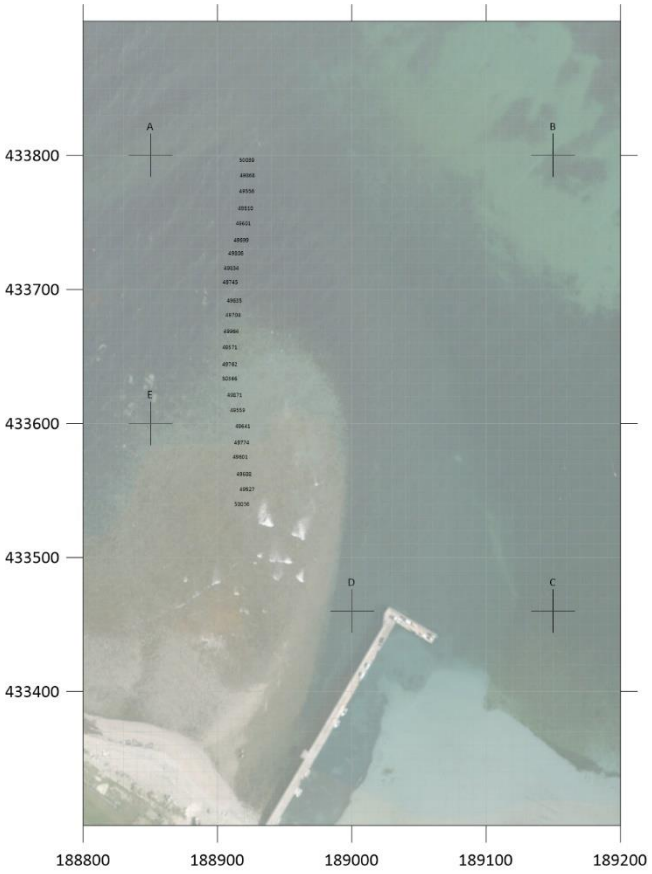


Figure 32

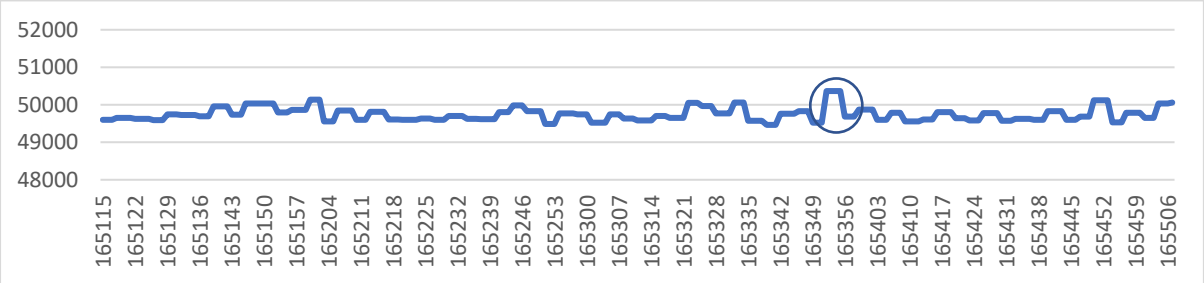


Figure 33. Line M-S10

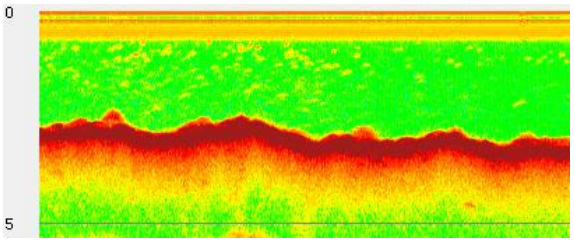


Figure 34. Sonar at 188909, 433634

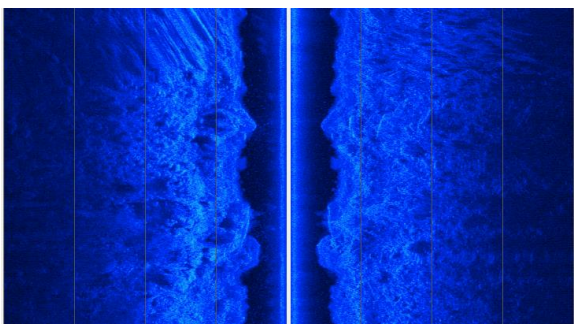


Figure 35. Side-scan Sonar at 188909, 433634

Line M-N11

Direction	North	
Offset	-10	Metres
Max	50377	nT
Median	49675	nT
Min	49450	nT
Start	165522	UTC
Finish	165905	UTC

Table 12

Line M-N11 centres on 188890 (Figure 32). This line (Figure 33) is entirely over the reef and demonstrates geological variations.

The interesting anomaly at 1655 (188890, 433600) was cross checked with sonar (Figure 34) and side-scan (Figure 35) and represents a small boulder field and some exposed bedrock. The anomalies at 1658 (188890, 433785) have also been verified as boulders and bedrock.

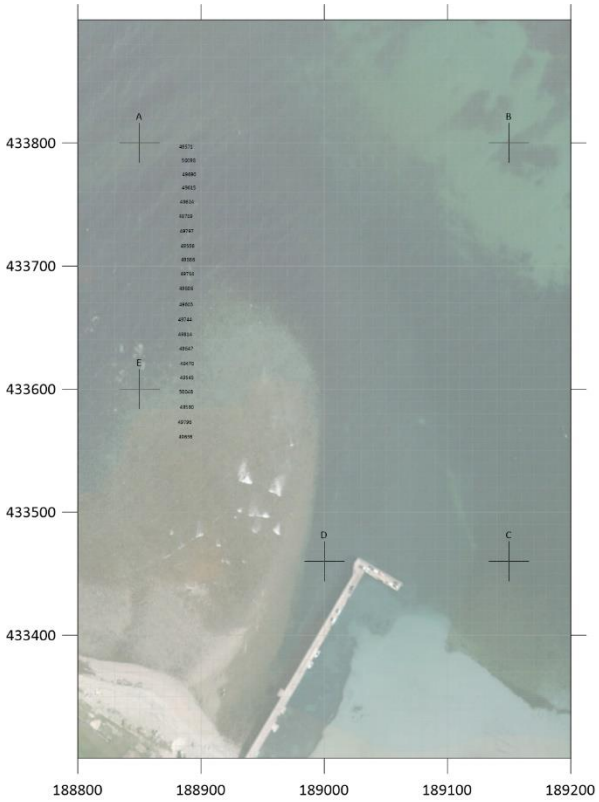


Figure 36

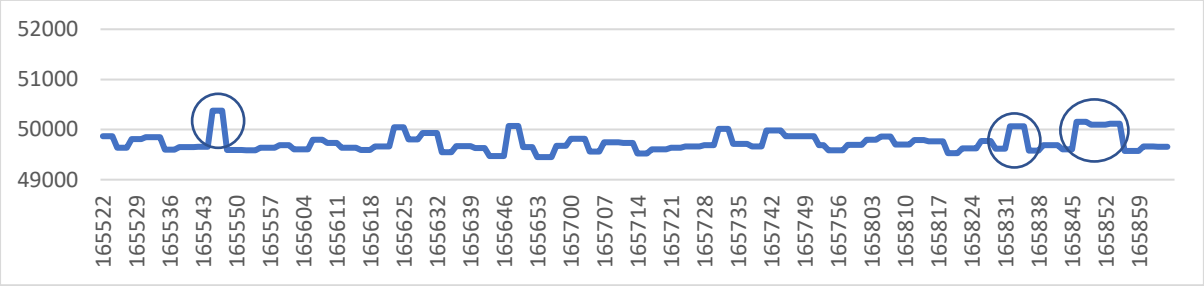


Figure 37. Magnetometer trace for line M-N11

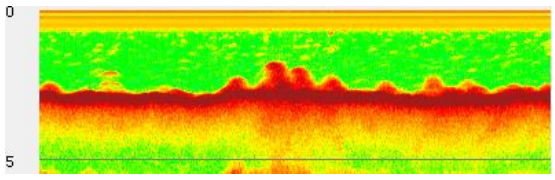


Figure 38. Sonar at 188890, 433600

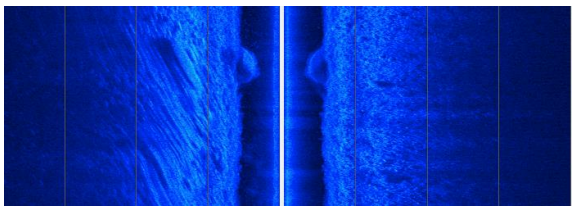


Figure 39. Side-scan Sonar at 188890, 433600

Line M-S12

Direction	South	
Offset	10	Metres
Max	50483	nT
Median	49771	nT
Min	49328	nT
Start	165919	UTC
Finish	170234	UTC

Table 13

Line M-S12 centres on 188870 (Figure 36). This line (Figure 37) is entirely over the reef and demonstrates geological variations.

The anomaly at 1659 (188870, 433798) was cross checked with sonar (Figure 38) and side-scan (Figure 39) and represents exposed bedrock.

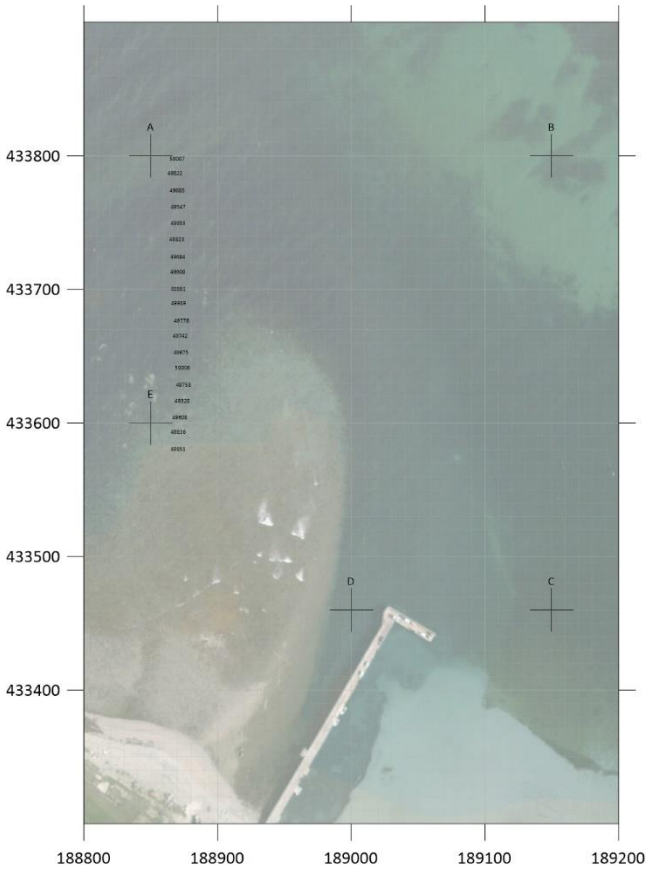


Figure 40

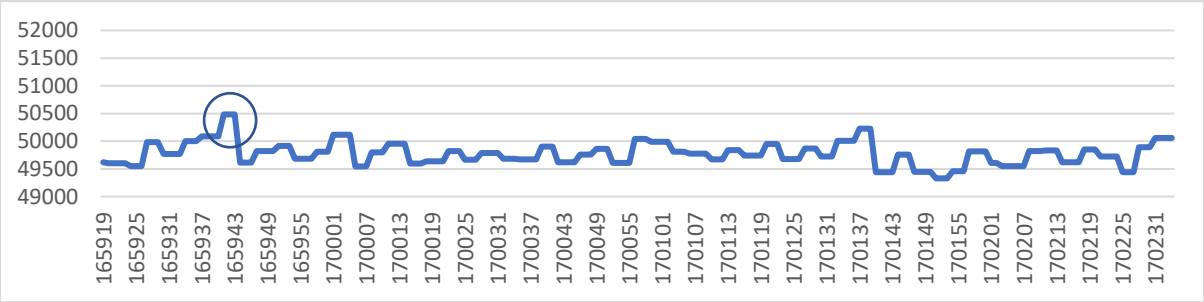


Figure 41. Magnetometer trace for line M-S12

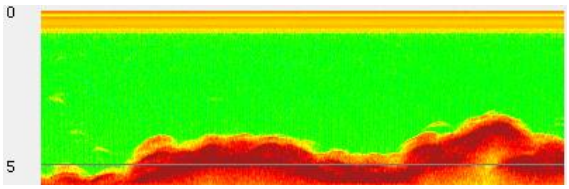


Figure 42. Sonar at 188870, 433798

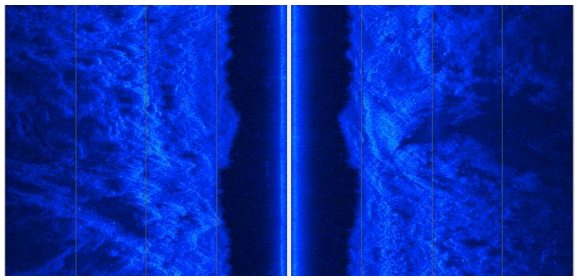


Figure 43. Side-scan Sonar at 188870, 433798

Line M-N13

Direction	North	
Offset	-10	Metres
Max	50384	nT
Median	49704	nT
Min	49445	nT
Start	170244	UTC
Finish	170608	UTC

Table 14

Line M-N13 centres on 188850 (Figure 40). This line (Figure 41) is entirely over the reef and demonstrates geological variations.

The anomalies at 1703 (188848, 433609) were cross checked with sonar (Figure 42) and side-scan (Figure 43) and represents a boulder field with exposed bedrock.

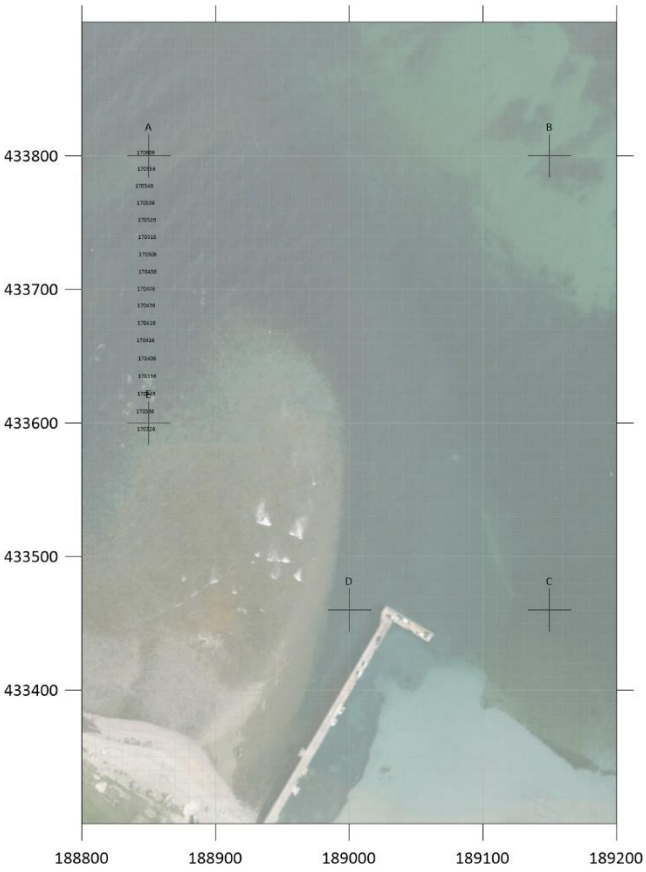


Figure 44

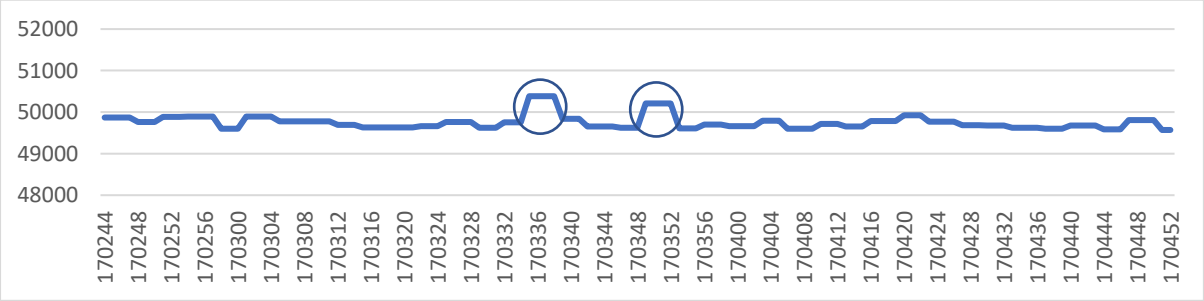


Figure 45. Line M-N13

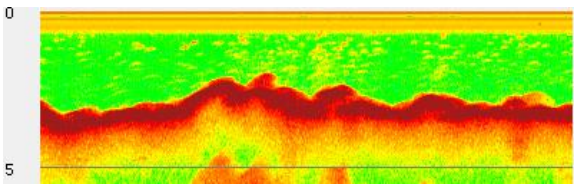


Figure 46. Sonar at 188848, 433609

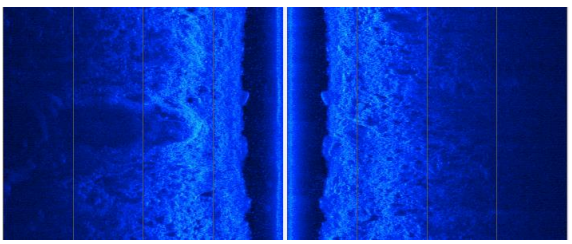


Figure 47. Side-scan Sonar at 188848, 433609

7. References

[1] https://www.magie.ie/